Petroleum Science 20 (2023) 20–33

Contents lists available at ScienceDirect

Petroleum Science

journal homepage: www.keaipublishing.com/en/journals/petroleum-science

Original Paper

Driving forces and their relative contributions to hydrocarbon expulsion from deep source rocks: A case of the Cambrian source rocks in the Tarim Basin

Bo Pang [a, b], Jun-Qing Chen [a, c, d, e, *], Xiong-Qi Pang [a, b, **], Tao Hu [a, b], Yue Sheng [f]

[a] State Key Laboratory of Petroleum Resources and Prospecting, China University of Petroleum, Beijing, 102249, China
[b] College of Geosciences, China University of Petroleum, Beijing, 102249, China
[c] College of Science, China University of Petroleum, Beijing, 102249, China
[d] Laboratory of Optical Detection Technology for Oil and Gas, China University of Petroleum, Beijing, 102249, China
[e] Basic Research Center for Energy Interdisciplinary, China University of Petroleum, Beijing, 102249, China
[f] CNPC Economics & Technology Research Institute, Beijing, 100029, China

ARTICLE INFO

Article history:
Received 19 October 2021
Received in revised form
26 May 2022
Accepted 11 August 2022
Available online 24 August 2022

Edited by Jie Hao and Teng Zhu

Keywords:
Driving force
Dynamic mechanism
Hydrocarbon expulsion
Deep oil and gas exploration
Tarim Basin

ABSTRACT

To thoroughly understand the dynamic mechanism of hydrocarbon expulsion from deep source rocks, in this study, five types of hydrocarbon expulsion dynamics (thermal expansion, hydrocarbon diffusion, compaction, product volume expansion, and capillary pressure difference (CPD)) are studied. A model is proposed herein to evaluate the relative contribution of different dynamics for hydrocarbon expulsion using the principle of mass balance, and the model has been applied to the Cambrian source rocks in the Tarim Basin. The evaluation results show that during hydrocarbon expulsion from the source rocks, the relative contribution of CPD is the largest (>50%), followed by compaction (10%–40%), product volume expansion (5%–30%), and thermal expansion (2%–20%). The relative contribution of diffusion to hydrocarbon expulsion is minimal (<10%). These results demonstrate that CPD plays an important role in the hydrocarbon expulsion process of deep source rocks. The hydrocarbon expulsion process of source rocks can be categorized into three stages based on the contribution of different dynamics to the process: the first stage is dominated by compaction and diffusion to expel hydrocarbons, the second stage is dominated by product volume expansion and CPD, and the third stage is dominated by product volume expansion and CPD. This research offers new insights into hydrocarbon exploration in tight oil and gas reservoirs.

1. Introduction

Tight oil and gas reservoirs are widely distributed in the deep tight reservoirs, accounting for more than 85% of the total unconventional oil/gas resources (Zou, 2014; Jia, 2017; Tong et al., 2018). Their great resource potential has attracted considerable attention from petroleum geologists and explorers for a long time (SPE et al., 2007; Jarvie, 2012; Jia, 2017; Zheng et al., 2019). Tight oil and gas reservoirs have completely different dynamics from those of conventional oil and gas reservoirs; therefore, the distribution of tight oil and gas reservoirs is mainly controlled by source rocks (Zou, 2014; Pang et al., 2021b; Hu et al., 2022). Considering that deep oil and gas reservoirs are widely distributed in tight reservoirs, most scholars believe that the hydrocarbon migration and accumulation in tight reservoir layers (Fig. 1) is driven by nonbuoyancy forces (Zou et al., 2012; Song et al., 2019; Jia et al., 2021). However, there are various types of nonbuoyancy forces and their effects on hydrocarbon expulsion are different.

Previous studies assumed that overpressure was the main driving force for hydrocarbon expulsion from source rocks (Dickinson, 1953; Hunt, 1990; Osborne and Swarbrick, 1997; Hao, 2005; Jiang et al., 2016). However, there are several formation mechanisms of overpressure, including product volume expansion,

* Corresponding author. State Key Laboratory of Petroleum Resources and Prospecting, China University of Petroleum, Beijing 102249, China.
** Corresponding author. State Key Laboratory of Petroleum Resources and Prospecting, China University of Petroleum, Beijing 102249, China.
E-mail addresses: 284289972@qq.com (B. Pang), chenjq@cup.edu.cn (J.-Q. Chen), pangxq@cup.edu.cn (X.-Q. Pang).

https://doi.org/10.1016/j.petsci.2022.08.011

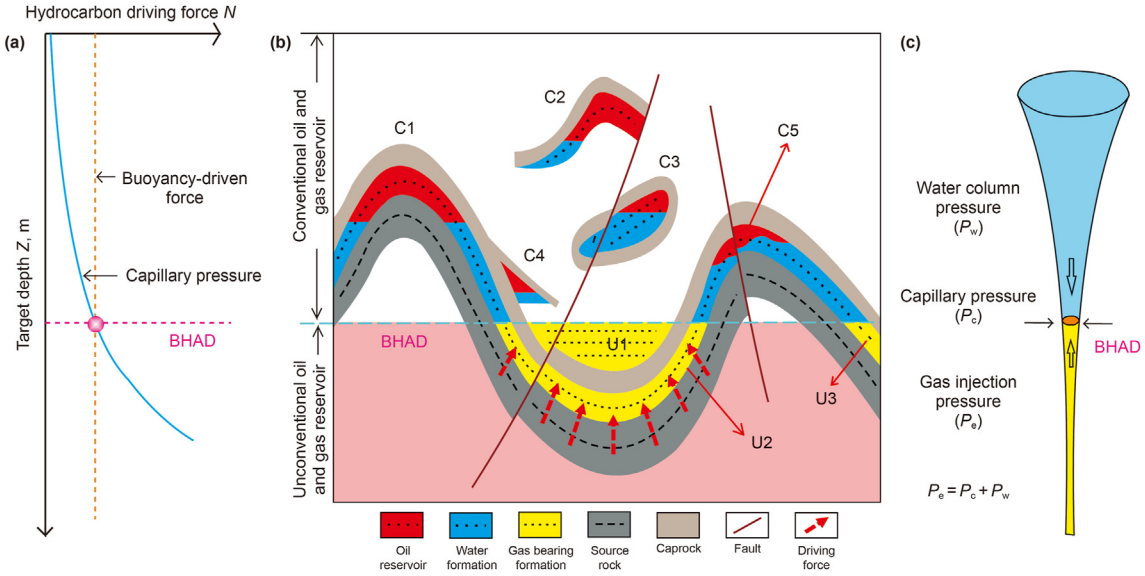

Fig. 1. Distribution of deep and tight reservoirs and their relation to buoyancy-driven hydrocarbon accumulation depth (BHAD) (quoted from Pang et al., 2021b). (a) Driving force of hydrocarbon migration is changed from buoyancy to nonbuoyancy with increasing depth. (b) Distribution of conventional and unconventional oil and gas resources and their relation to BHAD. (c) Decreases in the maximum pore throat radius in the target layer result in the transformation of hydrocarbon accumulation dynamic mechanisms from shallow reservoirs to deep and tight reservoirs. BHAD is defined as the critical condition corresponding to the change in the hydrocarbon driving force (Pang et al., 2021b).

thermal expansion, and compaction (Hao, 2005; Jiang et al., 2016). For evaluating the effect of different dynamics on hydrocarbon expulsion more accurately, the hydrocarbon expulsion dynamics are summarized based on Pang et al. (2000; 2001; 2021b) research. According to Pang's research, there were five types of dynamics and nine driving forces, i.e., compaction due to overlying strata (Lee et al., 2018), product volume expansion due to organic matter transformation (Espitalie et al., 1980) and clay mineral dehydration (Lindgreen, 1985), thermal expansion of minerals and fluids (water, oil, and gas) in source rocks (Magara, 1975a, 1975b; Barker, 1980; Olgaard et al., 1997), diffusion caused by the hydrocarbon concentration gradient (Leythaeuser et al., 1982), and capillary pressure difference (CPD) between surrounding source rocks and inner reservoirs (Magara, 1978; Stainforth and Reinders, 1990). The importance of these forces in hydrocarbon expulsion has been verified by several scholars (Chen and Tian, 1989; Pittman, 1992; Li, 2004; Qiao et al., 2019; Wang et al., 2022). However, the most important driving force among these nonbuoyancy forces in the process of hydrocarbon expulsion remains unclear. Currently, how to determine the dominant driving force in the process of hydrocarbon expulsion from source rocks is the most crucial problem for geologists.

Numerous studies have evaluated the importance of different hydrocarbon expulsion dynamics (Magara, 1978; Espitalie et al., 1980; Leythaeuser et al., 1982; Rose, 2001) and mainly focused on a single driving force (Lindgreen, 1985; Stainforth and Reinders, 1990). However, the study of single driving force cannot effectively reflect the effect of the driving force in the entire hydrocarbon expulsion process, resulting in incomplete understanding of the dynamics in the hydrocarbon expulsion process. Therefore, revealing dominant driving forces and quantitatively evaluating their contributions to hydrocarbon expulsion in deep areas is of practical significance for understanding the main controlling factors of hydrocarbon expulsion. This benefits explorations in tight reservoirs. Based on the abovementioned research purposes, herein, we focus on the differences and correlations of these driving forces in oil/gas expulsion from source rocks to quantify their relative contributions in a tight reservoir formation with increasing depth.

2. Geological setting

The Tarim Basin is rich in deep-seated oil and gas resources. Oil and gas are mainly concentrated in Paleozoic marine strata (Han et al., 2012; Zhu et al., 2012; Lan et al., 2015). The lithology of the target strata mainly presents carbonate rocks, including limestone and dolomite (Hu et al., 2015; Liu et al., 2015). The maximum depth of the oil and gas reservoirs is more than 8800 m, and their formation and distribution are mainly related to fault zones, unconformities, and reconstructed reservoirs (Fig. 2; Yu et al., 2012; Huang et al., 2016; 2016; Shen et al., 2018). These oil and gas reservoirs are mainly reformed as unconventional tight oil and gas reservoirs distributed near the source rocks (Shen et al., 2018). Therefore, the Tarim Basin is selected as the research object in our study to provide some suggestions for its deep exploration. The Paleozoic Middle–Lower Cambrian and Middle–Upper Ordovician source rocks are realized as the main source rocks in the deep area of the Tarim Basin (Li et al., 2010, 2015; Huang et al., 2016). The source rocks are mainly developed marine carbonate rocks and mudstones (Shen et al., 2018). In our study, the Cambrian source rocks are the main research objects.

3. Method and parameters

3.1. Classification of driving forces

Previous research works (Pang et al., 2001, 2021b) have studied the five types of dynamics (T1–T5) and nine driving forces (F1–F9) of hydrocarbon expulsion, and sufficient evidence of each driving force has been proposed (Magara, 1976; Berg, 1975; Magara, 1978; Espitalie et al., 1980; Leythaeuser et al., 1982; Lindgreen, 1985; Stainforth and Reinders, 1990; Rose, 2001). Fig. 3 presents the differences between these driving forces in the burial process of the source rocks.

Hydrocarbon diffusion (T1) is regarded as a type of dynamics for hydrocarbon expulsion from source rocks (Leythaeuser et al., 1982; Rose, 2001; Qiao et al., 2019), expressed as **F1**. However, the total amount of expelled hydrocarbon is limited because the

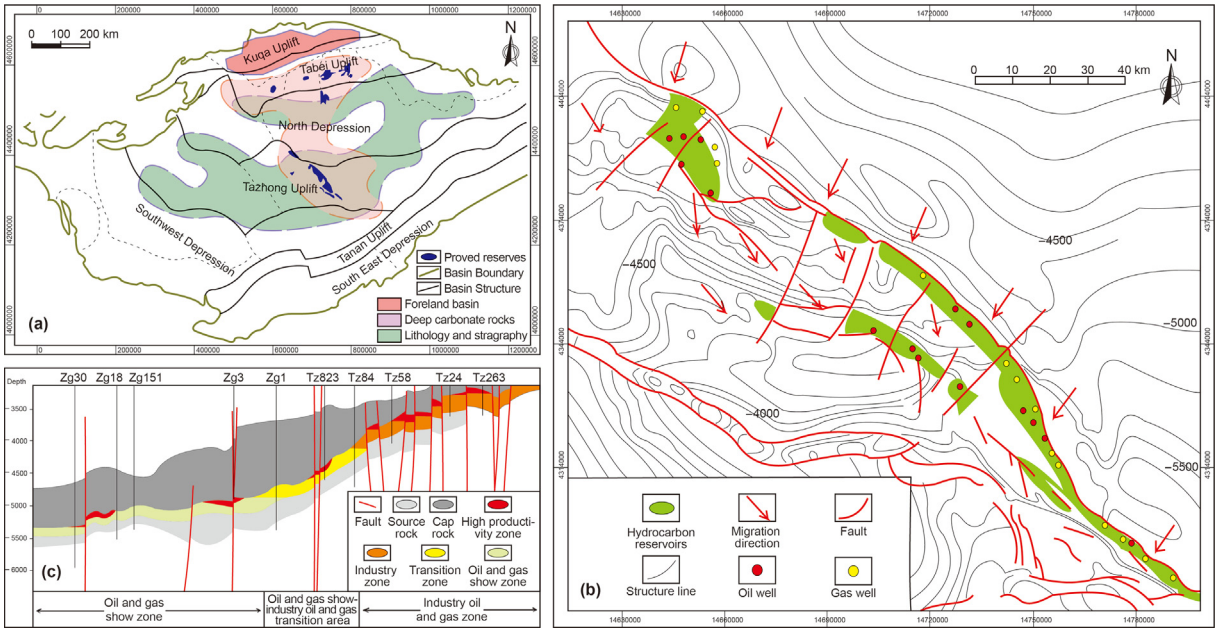

Fig. 2. Distribution characteristics of Paleozoic marine crude oil and its correlation with the Ordovician and Cambrian source rocks in the Tazhong Uplift, Tarim Basin. (a) Plane distribution characteristics of the oil and gas reservoirs. (b) Oil and gas reservoirs section (northwest to southeast). (c) Conceptual model of the oil and gas accumulation in the reservoirs of the trending section.

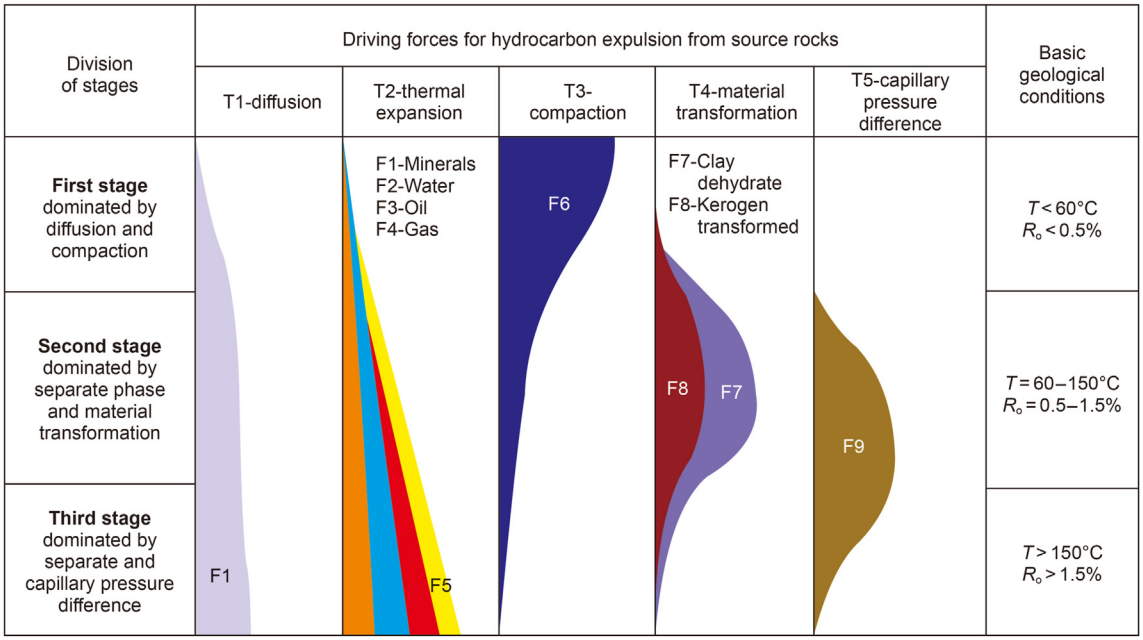

Fig. 3. Driving forces for hydrocarbon expulsion from the source rocks and variation characteristics of the hydrocarbon expulsion amount under the action of each type of force with increasing depth.

diffusion coefficient of hydrocarbons through rock media is very small (Leythaeuser et al., 1982).

The thermal expansion (T2) of minerals and fluids is another type of dynamics for hydrocarbon expulsion from source rocks (Olgaard et al., 1997). This type of dynamics can be subdivided into the thermal expansion of mineral skeleton (**F2**), water (**F3**), liquid oil (**F4**), and natural gas (**F5**) (Magara, 1975a, 1975b; Barker, 1980). The amounts of the expelled fluid or hydrocarbon are mainly related to the total amount of minerals, water, oil, and gas in the source rocks and their thermal expansion coefficients (Magara, 1975a, 1975b; Barker, 1980). The driving force increases with increasing burial depth and temperature. However, it may be mainly confined to the early and middle stages because the residual pore fluids (water, oil, and gas) in the source rocks are very little in deep strata (Magara, 1975a). In addition, the amount of hydrocarbon expelled due to mineral expansion is very limited because the thermal expansion coefficients of minerals are quite small (Barker, 1980).

The compaction of source rocks (T3) by overlying strata is also regarded as a type of dynamics for hydrocarbon migration (Magara,

1978; Lee et al., 2018), expressed as **F6**. As the porosity decreases because of compaction, the residual hydrocarbon saturation in the pores increases and free phase hydrocarbon is discharged in large quantities (Chen and Tian, 1989). The compaction may be mainly confined to the early stage of hydrocarbon expulsion in argillaceous source rocks and may not be as important in the middle and late stages with greater burial depth (Lee et al., 2018). In addition, its significance for hydrocarbon expulsion in the water-soluble phase may be greater than that in the other phase states. However, the amount of hydrocarbons expelled via compaction is very limited because the solubility of oil and gas in water is small (Price, 1976).

Product volume expansion (T4) through organic-parent-material pyrolysis transformation (Espitalie et al., 1980) and clay mineral dehydration (Magara, 1975a; Lindgreen, 1985) is regarded as the fourth type of dynamics for hydrocarbon expulsion, expressed as kerogen transformation to oil/gas (**F7**) and clay dehydration (**F8**). During the burial of source rocks, several material transformations result in an increase in volume, generating energy for discharging oil and gas (England et al., 1987). These transformations mainly occur in the middle stage of hydrocarbon expulsion from source rocks. However, their contribution to hydrocarbon expulsion in source rocks may be very limited owing to the small expansion coefficient (Espitalie et al., 1980; Lindgreen, 1985).

The CPD (T5) between the source rocks and the adjacent reservoirs is regarded as the fifth type of dynamics for hydrocarbon expulsion from source rocks (Berg, 1975), expressed as **F9**. Capillary forces have been considered as the resistance to hydrocarbon migration for a long time (Hubbert, 1953; Pittman, 1992). In 1987, England put forward the concept of interfacial potential (England et al., 1987), and scholars began to consider the CPD between source rocks and the surrounding rocks as the driving force for hydrocarbon migration (Berg RR, 1975; Dickey, 1975; Du, 1981; Pang et al., 2021b). However, the contribution of CPD remains controversial (Rouchet, 1981; Stainforth and Reinders, 1990). Some researchers believe that the effect of CPD on hydrocarbon migration and accumulation is very limited and should be neglected because of its small value (Dickey, 1975; Du, 1981; Li, 2004; Bao et al., 2017). Some believe that although CPD plays a very important role, it is limited to certain geological conditions in the evolution of source rocks when massive hydrocarbons are generated and organic networks are formed in a source rock (McAulife, 1979; England et al., 1987; Jia et al., 2021). Further, the contribution of CPD is considered to be confined in reservoirs with highly uneven pore structure characteristics, where oil and gas constantly migrate from small capillary pores to larger pores, leading to gradual oil and gas enrichment (Zou et al., 2012; Jiang et al., 2017; Pang et al., 2021a; Jia et al., 2021).

3.2. Simulation method

Previous studies have proven that each of the aforementioned five types of dynamics and nine driving forces (Pang et al., 2001; Pang et al., 2021) can lead to hydrocarbon expulsion from source rocks. However, various complicated phenomena can be involved in the process of hydrocarbon expulsion (Magara, 1976; Berg, 1975; Magara, 1978; Espitalie et al., 1980; Leythaeuser et al., 1982; Lindgreen, 1985; Stainforth and Reinders, 1990; Rose, 2001), implying that the five types of dynamics and nine driving forces of hydrocarbon expulsion can all simultaneously exist but make different contributions at different stages. On the basis of the principle of material balance, the relative contributions of the nine forces are determined via numerical simulations using the following five steps (Fig. 4).

The first step is to study the evolution history of petroliferous basins and calculate the amount of hydrocarbon generation, retention, and expulsion from source rocks (Pang et al., 2016).

The second step is to estimate the amount of hydrocarbon expulsion from the following four phases of source rocks and their changing histories (Johnson, 1912). The oil/gas amounts expelled (Q_e) from source rocks in the water-soluble phase (Q_{ew}) (Price, 1976), diffusion phase (Q_{ed}) (Leythaeuser et al., 1982; Thomas and Clouse, 1990), oil-soluble phase (Q_{eog}) (Neglia, 1979), and free phase (Q_{es}) (Dickey, 1975) are hereby studied.

The third step is to study the oil/gas expulsion mechanisms of the nine driving forces and calculate the fluid volume ($\triangle Q_f, f = 1, 2, \ldots,9$) expelled from the source rocks by each driving force.

The fourth step is to calculate the amount of hydrocarbon (Q_{ef}, $f = 1, 2, \ldots, 9$) expelled via the nine driving forces according to their expelled fluid volumes and relationships to oil/gas amounts expelled from the four phases. The amount of hydrocarbon expelled in the diffusion phase (Q_{ed}) was only related to F1 and that involved in the water-soluble phase (Q_{ew}) was associated with F2–F8. The amounts of hydrocarbons in the oil-solution phase (Q_{eo}) and the free phase (Q_{es}) are contributed by F2–F9. The total expelled hydrocarbon quantity (Q_{ef}) for all driving forces is the sum of the oil/gas amount expelled in the four phases, which could be denoted as $Q_{ef} = Q_{edf} + Q_{ewf} + Q_{eof} + Q_{esf}$, $f = 1, 2, 3, \ldots, 9$.

The fifth step is to evaluate the relative contribution (K_f) of each driving force (f) to all the oil/gas amounts expelled from source rocks in different phases during a certain depth interval, denoted as $K_f = Q_{ef}/\sum(Q_{eif})$, $f = 1, 2, \ldots 9$. The value of $\sum(Q_{ei})$ refers to the sum of the cumulative hydrocarbon amounts expelled by the nine driving forces in the four phases. The variations in Q_{ef} and K_f with the increasing burial depth of source rocks were calculated at 250 m depth intervals.

F1 is the diffusion force for hydrocarbon expulsion from source rocks. F2–F5 are the thermal expansion forces of mineral skeleton, water, liquid oil, and natural gas. F6 is the compaction stress from overlying strata. F7 and F8 occur due to pressures from increasing fluid volumes caused by clay dehydrates and kerogen transformation to oil/gas. F9 is the CPD between the source rocks and the surrounding rocks. $\triangle Q_{f2}$–$\triangle Q_{f8}$ are the fluid volumes expelled by driving forces F2–F8. Q_{ef1}–Q_{ef9} are the oil/gas amounts expelled by driving forces F1–F9. K_j is the relative contributions of each driving force Fj, $j = 1, 2, \ldots, 9$.

3.2.1. Simulation of hydrocarbon expulsion amounts from source rocks

The following numerical simulation is based on the recovery of the burial history and thermal evolution of the source rocks, and relevant methods can be found in previous studies (Lerche, 1990; Pang et al., 1993, 2001).

The generated hydrocarbon's amount depends on the quality and maturity of the source rocks. According to the principle of mass balance, the generated hydrocarbon amount (Q_p) per cubic meter of source rock (Pang et al., 1993, 2001) is denoted as follows:

$$Q_p = R_p(R_o,\ KTI) \cdot D(Z) \cdot TOC(R_o,\ KTI)/100, \quad (1)$$

where Q_p is the total amount of hydrocarbon generated per cubic meter of source rock (in kg/m^3 for oil and m^3/m^3 for gas), $R_p(R_o, KTI)$ refers to the hydrocarbon amount generated per unit weight of organic matter (in kg/t for oil and in m^3/t for gas), whose quantitative relationship has already been established (Tissot and Welte, 1978; Hunt, 1979), $D(Z)$ is the source-rock density (t/m^3), which varies with depth (Z) (Magara, 1981), and TOC is the original total organic carbon content (%). The generated hydrocarbon components are divided into three groups: liquid oil (C_n, $n \geq 6$), heavy hydrocarbon gas (C_{2-5}), and methane gas (C_1).

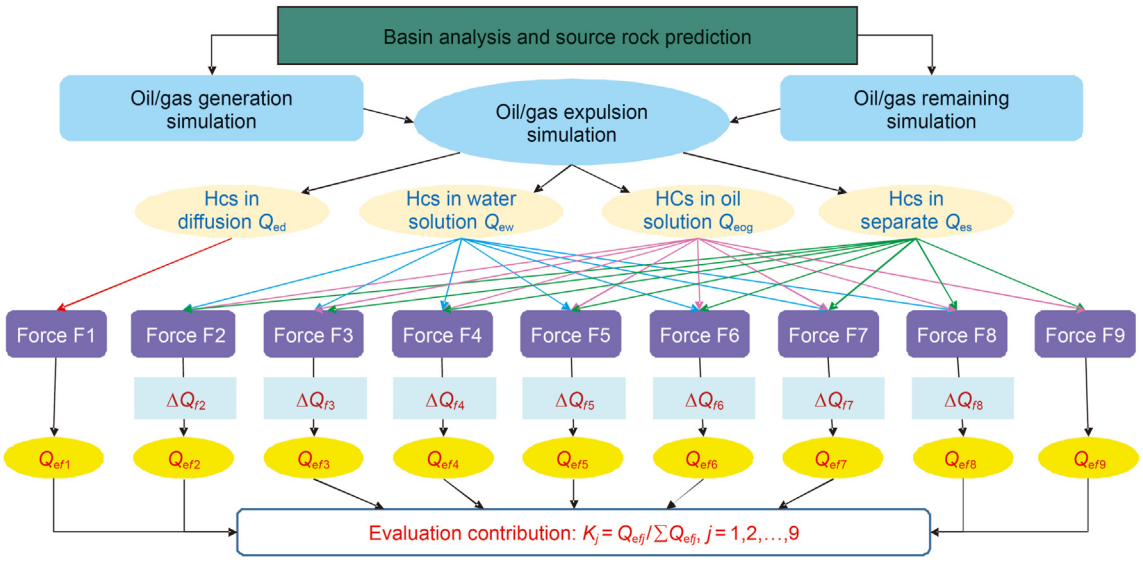

Fig. 4. Technologies for evaluating the contributions of nine driving forces to oil/gas expulsion from source rocks and their workflow.

The calculation model of the total residual oil amount is modified based on the report by Pang et al. (2001) and expressed as Eq. (2):

$$Q_{ro} = \rho_o \cdot (\varphi_n + \Delta\varphi) \cdot (A_0 + A_1 \cdot (TOC) + A_2 \cdot (TOC)) \cdot \frac{1}{1 - B_k} \cdot e^{-\frac{\varphi_n}{D}(R_o - R')^2}, \quad (2)$$

where Q_{ro} refers to the total amount of residual oil per cubic meter of source rock (kg/m^3), φ_n is the porosity of source rocks with normal compaction (%), and $\Delta\varphi$ is the extra porosity of source rocks with abnormal compaction (%). R_o refers to the critical vitrinite reflectance corresponding to the maximum value of the residual hydrocarbon peak (%). ρ_o denotes the crude oil density (t/m^3). A_0, A_1, A_2, and D denote the constant values determined through statistical analysis (Behar et al., 2001) with the best fitness between the actual data "S_1" or "A" with the calculation model (Pang et al., 2001). B_k is the light-hydrocarbon compensation factor (Chen et al., 2018), which is quantitatively related to major factors established before (Pang et al., 1993).

The total residual gas amount in the source rocks can be divided into three types and calculated using Eq. (3):

$$Q_{rg} = \left(Q_{rgb} + Q_{rgo} + Q_{rgw} + Q_{rs}\right) \quad (3)$$

where Q_{rg} is the total amount of residual gas per cubic meter of source rock (m^3/m^3), including the adsorbed gas amount of Q_{rgb} (Qu et al., 2020), oil-dissolved gas amount of Q_{rgo} (He et al., 2020), water-dissolved gas amount of Q_{rgw} (Li et al., 2018), and free gas amount of Q_{rs} (Rexer et al., 2013).

Similarly, according to the principle of material balance, the amount of hydrocarbon expulsion from source rocks in different phases can be calculated (Pang et al., 2001) using Eq. (4):

$$Q_e = R_e(R_o, KTI) \cdot D(Z) \cdot TOC(R_o, KTI)/100, \quad (4)$$

where Q_e is the total hydrocarbon expulsion amount per cubic meter of source rock (in kg/m^3 for oil and in m^3/m^3 for gas) and $R_e(R_o, KTI)$ is the amount of hydrocarbon expelled per unit weight of organic matter (in kg/t for oil and in m^3/t for gas), which changes with KTI and R_o (Pang et al., 2005; Jiang et al., 2016).

The hydrocarbon expulsion threshold (HET) of the source rocks can be determined using Eq. (5), which corresponds to the critical conditions (Pang et al., 2020, 2021a) where the generated hydrocarbon amount (Q_p) is equal to the residual hydrocarbon amount (Q_{rm}):

$$Q_p \geq Q_{rm} = Q_{ro} + Q_{rg} \quad (5)$$

3.2.2. Simulation of hydrocarbon expulsion from source rocks in different phases

The phase states of the oil and gas expelled from source rocks can be mainly divided into four phases: the diffusion phase (Price, 1976), water-soluble phase (Leythaeuser et al., 1982), oil-soluble phase (Neglia, 1979), and free phase (Dickey, 1975).

The amount of hydrocarbon expelled from source rocks in the water-soluble phase can be calculated (Leythaeuser et al., 1982) using Eq. (6):

$$Q_{ew} = V_{ew} \cdot \sum_{1}^{4} q_{ew}(i) \quad (6)$$

where Q_{ew} is the amount of hydrocarbon expelled as a water-soluble (in kg/m^3 for oil and in m^3/m^3 for gas), changing with the water volume expelled from source rocks (V_{ew}), hydrocarbon component (i), and hydrocarbon solubility in water (q_{ew}). q_{ew} is controlled by the oil/gas component (i), temperature (T), pressure (P), and water mineralization (X_k), and their relationships can be confirmed (Price, 1976).

The amount of hydrocarbon expelled from source rocks in the diffusion phase can be calculated (Price, 1976) using Eq. (7):

$$Q_{ed} = \sum_{1}^{4} \int_{0}^{t} D(i, T, \varnothing) \cdot \frac{dc}{dz} \cdot dt \quad (7)$$

where Q_{ed} refers to the amount of hydrocarbon expelled as the diffusion phase (in kg/m^3 for oil) and in m^3/m^3 for gas), changing with the source-rock distribution areas (S), diffusion time (t), inside hydrocarbon composition (i), concentration gradient (dc/dz), and

diffusion coefficient D (i, T, Φ). The relationships of the diffusion coefficient with hydrocarbon components (i), temperature (T), and medium porosity (Φ) are determined (Leythaeuser et al., 1982).

The amount of hydrocarbon expelled from source rocks as an oil-solution phase can be calculated (Neglia, 1979) using Eq. (8).

$$Q_{eog} = Q_{eo} \cdot \sum_{1}^{4} q_o(i) \tag{8}$$

where Q_{eog} denotes the amount of gas expelled from source rocks as an oil-solution phase (in kg/m^3 for oil and in m^3/m^3 for gas), changing with the amount of expelled oil and the solubility of the gas in the oil (q_o). The relationships of q_o and the gas component (i), temperature (T), pressure (P), and oil density (ρ_o) were determined by Bruce (1984).

The amount of hydrocarbon expelled from source rocks in the free phase can be calculated (Dickey, 1975) using Eq. (9):

$$Q_{es} = Q_e - Q_{ew} - Q_{ed} - Q_{eog} \tag{9}$$

where Q_{es} is the amount of hydrocarbon expelled in the free phase (in kg/m^3 for oil and in m^3/m^3 for gas), changing with the total hydrocarbon expulsion amount from the source rocks (Q_p–Q_{rm}). The hydrocarbon expulsion amount from the source rocks in the free phase is most significant for oil/gas accumulation (Magara, 1978).

Further, the characteristics of hydrocarbon expulsion from source rocks during the evolution of source rock can be analyzed. These characteristics can be expressed as the following parameters: velocity (V_e), rate (S_e), and efficiency (R_e) of hydrocarbon expulsion and the source-rock index (*SRI*). These key parameters for hydrocarbon expulsion at different depth intervals are calculated using Eqs. (10)–(13):

$$V_e = \frac{\Delta Q_e}{\Delta Z} \tag{10}$$

$$S_e = \frac{\Delta Q_e}{H} \tag{11}$$

$$R_e = \frac{Q_e}{Q_p}, \text{ and} \tag{12}$$

$$SRI = \frac{Q_{es}}{Q_e} \tag{13}$$

where V_e is the hydrocarbon expulsion velocity, changing with ΔQ_e and depth, S_e is the hydrocarbon expulsion rate, changing with V_e and the thickness of the source rocks (H), and R_e is the hydrocarbon expulsion efficiency, changing with different depths of the source rocks. *SRI* changes with the total oil/gas amount expelled from source rocks in the free phase (Q_{es}) and the total oil/gas amount expelled in different phases (Q_e).

3.2.3. Simulation of the relative contribution of different dynamics to hydrocarbon expulsion

The amount of hydrocarbon expelled in the diffusion phase (Q_{ed}) is controlled by the driving force F1. The hydrocarbon amount expelled from source rocks in the water-soluble phase (Q_{ew}) is controlled by the combination of seven driving forces (F_i, $i = 2$–8). Furthermore, the oil/gas amounts expelled in the oil-solution (Q_{eog}) and free (Q_{es}) phases are related to these eight driving forces (F_i, $i = 2$–9). The volumes of the liquid expelled from the source rocks due to different dynamics were calculated first to compare the relative magnitudes of various hydrocarbon expulsion dynamics.

The liquid volume expelled from source rocks owing to different driving forces can be calculated as follows (Pang et al., 2001). The volumes of the fluids expelled by seven driving forces are denoted as ΔV_{fi}, $i = 2, 3, \ldots, 8$.

The volumes of the liquid expelled by thermal expansion can be calculated using Eqs. (14)–(17) (Pang et al., 2001, 2003).

$$V_{f2} = (K_{sr2} - K_{sr1}) \cdot (1 - \Phi_0) \tag{14}$$

$$V_{f3} = (K_{hw2} - K_{hw1}) \cdot \left(\frac{\varphi_0 - \varphi_2}{1 - \varphi_2} - \frac{\varphi_0 - \varphi_1}{1 - \varphi_1}\right) \tag{15}$$

$$V_{f4} = (K_{ho2} - K_{ho1}) \cdot \left(\frac{\varphi_0 - \varphi_2}{1 - \varphi_2} - \frac{\varphi_0 - \varphi_1}{1 - \varphi_1}\right) \cdot S_o, \text{ and} \tag{16}$$

$$V_{f5} = \left(K_{hg2} - K_{hg1}\right) \cdot \left(\frac{\varphi_0 - \varphi_2}{1 - \varphi_2} - \frac{\varphi_0 - \varphi_1}{1 - \varphi_1}\right) \cdot S_G \tag{17}$$

where ΔV_{f2} is the volume of liquid expelled via the thermal expansion of mineral skeleton. K_{sr} is related to the expansion coefficient of the skeleton content ($1 - \Phi_0$) (David et al., 1997). ΔV_{f3} is the volume of liquid expelled via the thermal expansion of water, which is related to the source-rock porosity (Φ) and water expansion coefficient (K_{hw}) (Barker, 1980). ΔV_{f4} is the volume of liquid expelled via the thermal expansion of oil, which is related to the source-rock porosity (Φ), oil expansion coefficient (K_{ho}), and oil saturation (S_o) in source rocks (Magara, 1976). ΔV_{f5} is the volume of liquid expelled via the thermal expansion of gas, which is related to the variation of the source-rock porosity (Φ) and the gas-expansion coefficient (K_{hg}) (Magara, 1976).

The volumes of liquid expelled via compaction can be calculated using Eq. (18) (Pang et al., 2001, 2003).

$$V_{f6} = \left(\frac{\varphi_0 - \varphi_2}{1 - \varphi_2} - \frac{\varphi_0 - \varphi_1}{1 - \varphi_1}\right) \cdot H, \tag{18}$$

where ΔV_{f6} is the volume of liquid expelled via compaction and is related to porosity (Φ) and thickness of source rock (H) (Lee et al., 2018).

The volumes of liquid expelled via product volume expansion can be calculated using Eqs. (19) and (20) (Pang et al., 2001, 2003).

$$V_{f7} = (D_1 - D_2) \cdot (TOC_2 - TOC_1) \cdot K_v \tag{19}$$

$$V_{f8} = 0.245 \cdot \left(C_{lay2} - C_{lay1}\right) \cdot (I_{m2} - I_{m1}) \cdot (D_2 - D_1) \tag{20}$$

where ΔV_{f7} is the volume of liquid expelled via kerogen transformation, which is related to *TOC*, the density of source rocks (D), and the volume-increase coefficient (K_v) (Vernik and Landis, 1996). ΔV_{f8} is the volume of liquid expelled via clay dehydration, which is associated with the total content of clay minerals (C_{lay}) and secondary illites (I_m) formed via clay diagenesis and the volume-increase coefficient (England et al., 1987).

According to the volume of liquid expelled from source rocks owing to different dynamics, the relative magnitude of various hydrocarbon expulsion dynamics can be calculated using the modified Darcy's law (Germann, 2018) using Eq. (21).

$$F_i = \left[\frac{\mu H}{KS} \cdot \frac{dV_i}{dt}\right] \cdot 10^{12} \ (i = 2, 3, \ldots\ldots, 8) \tag{21}$$

where F_i is the relative magnitude of different hydrocarbon expulsion dynamics, μ is the fluid viscosity, which is replaced by

water viscosity because the water volume is the highest among the expelled fluid volume, accounting for 70% (Zheng et al., 2020), and H, K, and S represent the thickness, permeability, and area of the source rocks, respectively.

The relative magnitude of the ninth driving force ($F9$) can be calculated (McAulife, 1979; England et al., 1987) using Eqs. (22) and (23).

$$F_{9o} = Pc_{w/o} = 2 \cdot \delta_{w/o} \cdot \cos\theta \cdot \left(\frac{1}{r} - \frac{1}{R}\right) \tag{22}$$

$$F_{9g} = Pc_{w/g} = 2 \cdot \delta_{w/g} \cdot \cos\theta \cdot \left(\frac{1}{r} - \frac{1}{R}\right) \tag{23}$$

where Pc is the CPD between the source and surrounding rocks, r is the throat radius of surrounding rocks, R is the throat radius of reservoirs, and θ is the wetting angle of hydrocarbon/water. The capillary pressure differences between oil (F_{9o}) and gas (F_{9g}) are calculated separately.

According to the relationship between the hydrocarbon expulsion dynamics and the phase state of hydrocarbon expulsion, combined with the relative magnitude of the hydrocarbon expulsion dynamics, the relative contribution of different hydrocarbon expulsion dynamics to the amount of hydrocarbon expulsion was calculated.

The hydrocarbon amount of Q_{ed} expelled via F_1 is denoted as Q_{e1} and calculated (Leythaeuser et al., 1982) using Eq. (24).

$$Q_{e1} = D \cdot \frac{dc}{dz} \cdot \frac{1-\varphi_0}{1-\varphi_2} \cdot s \cdot \varphi_2 \cdot \Delta t \tag{24}$$

where D is the diffusion coefficient, dc/dz is the hydrocarbon concentration gradient, S is the diffusion area, φ is the porosity of the source rocks, and t is the diffusion period.

The amount of hydrocarbon expelled (Q_{ei}) via each of the other eight driving forces is calculated using Eq. (25). Q_{ew} is expelled owing to the combination of $\sum F_i$, $i = 2, 3, \ldots, 8$, whereas Q_{eog} and Q_{es} are expelled because of the combination of $\sum F_i$, $i = 2, 3, \ldots, 9$.

$$Q_{ei} = (Q_{es} + Q_{eog})/F_i + Q_{ew}/F_j \ (j = 2, 3, \ldots\ldots, 8;\ i = 2, 3, \ldots, 9). \tag{25}$$

Finally, the relative contributions of each driving force are obtained using Eq. 26.

$$R_i = \frac{Q_{ei}}{\sum_{i=1}^{9} Q_{ei}} \ (i = 2, 3, \ldots\ldots, 8). \tag{26}$$

3.3. Model parameters

The basic parameters of the Cambrian source rocks in the Tarim Basin must be obtained to accurately simulate their hydrocarbon expulsion processes. The source-rock parameters required in the abovementioned simulations mainly include the following five types of data: the thickness of the source rocks (H), total organic carbon (TOC) of the source rocks, kerogen type index (KTI), thermal evolution degree (R_o) or burial depth (Z), and thermal gradient. The characteristics of these parameters are illustrated in Fig. 5 and Table 1. Under the given geological conditions, H ranges from 0 to 450 m, with an average of ~200 m, TOC changes from 0.2% to 3.3%, with an average of 1.5%, KTI changes from 50 to 100, with an average of 85, the equivalent R_o changes from 0.8% to 4.1%, with an average of 1.8%, and the thermal gradient changes from 2.3 to 2.7 °C/100 m, with an average of 2.5 °C/100 m.

In addition to considering actual geological conditions, studying the amounts of hydrocarbon expulsion under various dynamic effects of source rocks involves a series of calculation parameters. These include the rock heat-expansion coefficient (Magara, 1975b), hydrocarbon heat-expansion coefficient (Magara, 1975a), hydrocarbon diffusion coefficient (Leythaeuser et al., 1984), natural gas–adsorption coefficient (Danial and Bustin, 2007), dissolution coefficient of hydrocarbon in water (Price, 1976), dissolution coefficient of gas in oil (Neglia, 1979), volume expansion coefficient of kerogen products (Espitalie et al., 1980), and clay mineral dehydration (Dickinson, 1953). These parameters used in the abovementioned equations are obtained from previous studies and listed in Table 2. Using the obtained geological condition data and parameters, the hydrocarbon expulsion model of the Cambrian source rocks in the Tarim Basin can be established accurately.

4. Results

4.1. Hydrocarbon expulsion in four phases from source rocks

Fig. 6 illustrates the case study results of hydrocarbon expulsion from the source rocks of the Tarim Basin in four different phases. Fig. 6a shows the variation characteristics of hydrocarbon generation, retention, and expulsion with increasing depth for methane; heavy gas; liquid hydrocarbons ; and SRI, clarifying the relationship of the generated, retained, and expelled oil/gas amounts per cubic meter in the evolution of source rocks. Fig. 6b shows the variation characteristics of hydrocarbon expulsion per cubic meter of source rocks with increasing depth. The oil/gas expulsion is characterized by four parameters: the accumulatively expelled hydrocarbon amount, hydrocarbon expulsion velocity, hydrocarbon expulsion rate per 100-m-depth-interval increase, and oil/gas expulsion efficiency. Fig. 6c shows the variation of relative amounts (%) of hydrocarbon expelled from source rocks in the four phases at the same depth intervals, including those for methane gas, heavy hydrocarbon gas, and liquid hydrocarbon.

4.2. Relative contributions of the nine driving forces to oil/gas expulsion

Fig. 7 presents the variation characteristics of the total water, natural gas (methane and heavy gas), and liquid oil expelled per cubic meter of source rocks by the nine driving forces with increasing depth. Fig. 7a shows the variation characteristics of the expelled water amount, expressed as instantaneous amounts per 100-m-depth intervals (a1), relative amounts (a2), and cumulative amounts (a3). Fig. 7b shows the variation characteristics of the expelled gas amount, expressed as instantaneous amounts per 100-m-depth intervals (b1), relative amounts (b2), and cumulative amounts (b3). Fig. 7c shows the variation characteristics of the expelled liquid-oil amounts expressed as instantaneous amounts (c1), relative amounts (c2), and cumulative amounts (c3). The total amount of water expelled from the source rocks is mainly related to compaction (50%), clay dehydration (35%), the thermal expansion of rock skeleton and fluids (9%), and kerogen transformation (6%). Compaction (F6) made the largest contribution to water expulsion, whereas CPD made the largest contribution to gas expulsion (>80%). Meanwhile, the contribution of diffusion was ~5%, while those of clay dehydration and kerogen transformation was 5% in total, and the compaction (4%) and thermal expansion of rock skeleton and fluids (<5%) had the smallest contributions. The contributions of the nine driving forces to the expelled oil amount were almost the same as the contributions to the expelled gas amount, which was mainly dominated by CPD (>85%), compaction

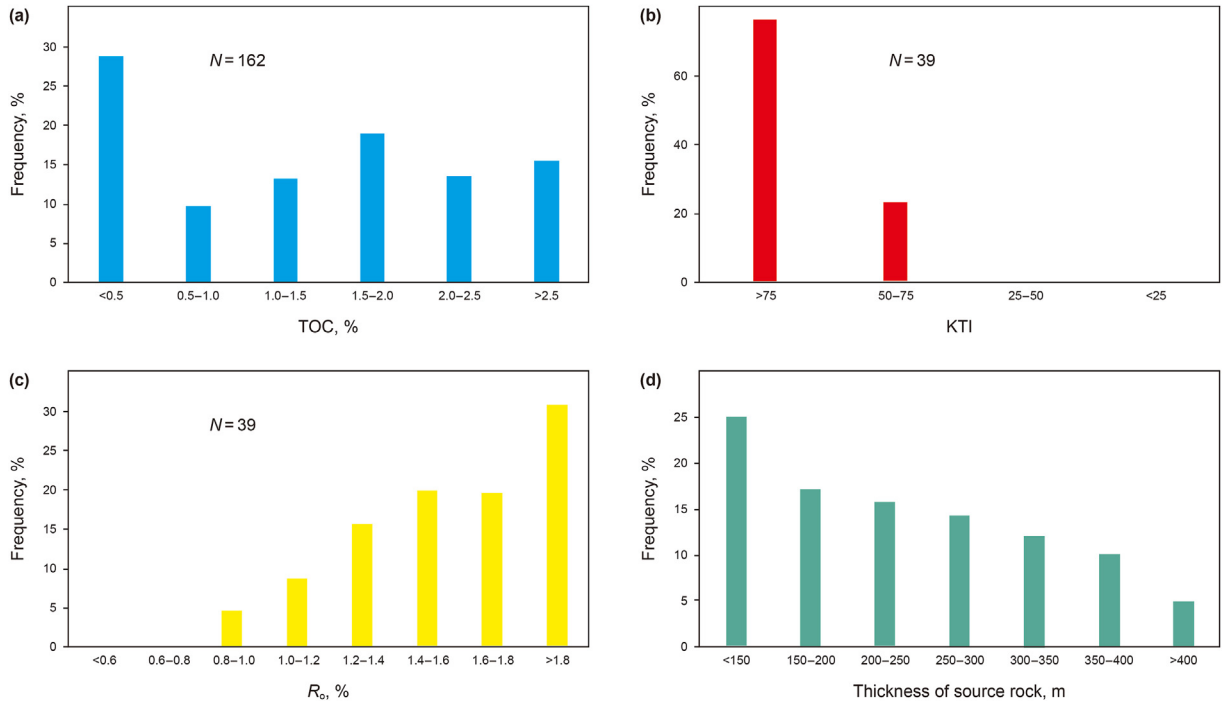

Fig. 5. Distribution characteristics of the geochemical and geological parameters of the Cambrian source rocks in the Tarim Basin. (a) Total organic carbon (%). (b) Organic-parent-material type (*KTI*). (c) Organic maturity degree of the equivalent vitrinite reflectance (%). (d) Thickness of source rocks (m).

Table 1
Geological parameters of the Cambrian source rocks in the Tarim Basin.

Geological Data	Source-rock thickness (m)	Total organic carbon (*TOC*), %	Kerogen type index (*KTI*)	Maturity (R_o), %	Thermal gradient, °C/100 m
Maximum	450	0.2	50	0.8	2.7
Minimum	0	3.3	97	4.1	2.3
Mean	200	1.5	85	1.8	2.5
Source	Li et al. (2010), 2015; Shen et al. (2018)	Li et al. (2010), 2015; Shen et al. (2018)	Pang et al. (1992); Li et al. (2010), 2015	Li et al. (2010), 2015; Shen et al. (2018)	Han et al. (2012); Hu et al. (2015); Liu et al. (2015)

Table 2
Sources of the driving force parameters.

Driving force parameters		Sources
Diffusion coefficient		Leythaeuser et al. (1982)
Thermal expansion coefficients	Rock	Magara, 1975b
	Water	Barker (1980)
	Liquid oil	Magara (1975a)
	Natural gas	Magara (1975a)
Volume expansion coefficient	Kerogen products	Espitalie et al. (1980)
	Clay mineral dehydration	Dickinson, 1953
Natural gas–adsorption coefficient		Danial and Bustin, 2007
Hydrocarbon dissolution coefficient in water		Price (1976)
Gas dissolution coefficient in oil		Neglia, 1979

(7%), clay and kerogen transformation (5%), and the thermal expansion of rock skeleton and fluids (<3%). As shown by the numerous simulation results obtained using various geological parameters, the contribution of CPD to the total expelled oil/gas amount was more than 50% with *TOC* > 0.5% and R_o > 0.5%, and its relative contribution increased with increasing depth. This implies CPD's dominant role in the formation and distribution of deep and tight oil/gas reservoirs.

4.3. Dynamic model for oil/gas expulsion from source rocks with increasing depth

The dynamic process of hydrocarbon expulsion from source rocks is divided into four stages with increasing depth, showing that different forces expel hydrocarbons from source rocks in different phases at different stages and make different contributions to oil and gas accumulations in deep and tight reservoirs (Fig. 8).

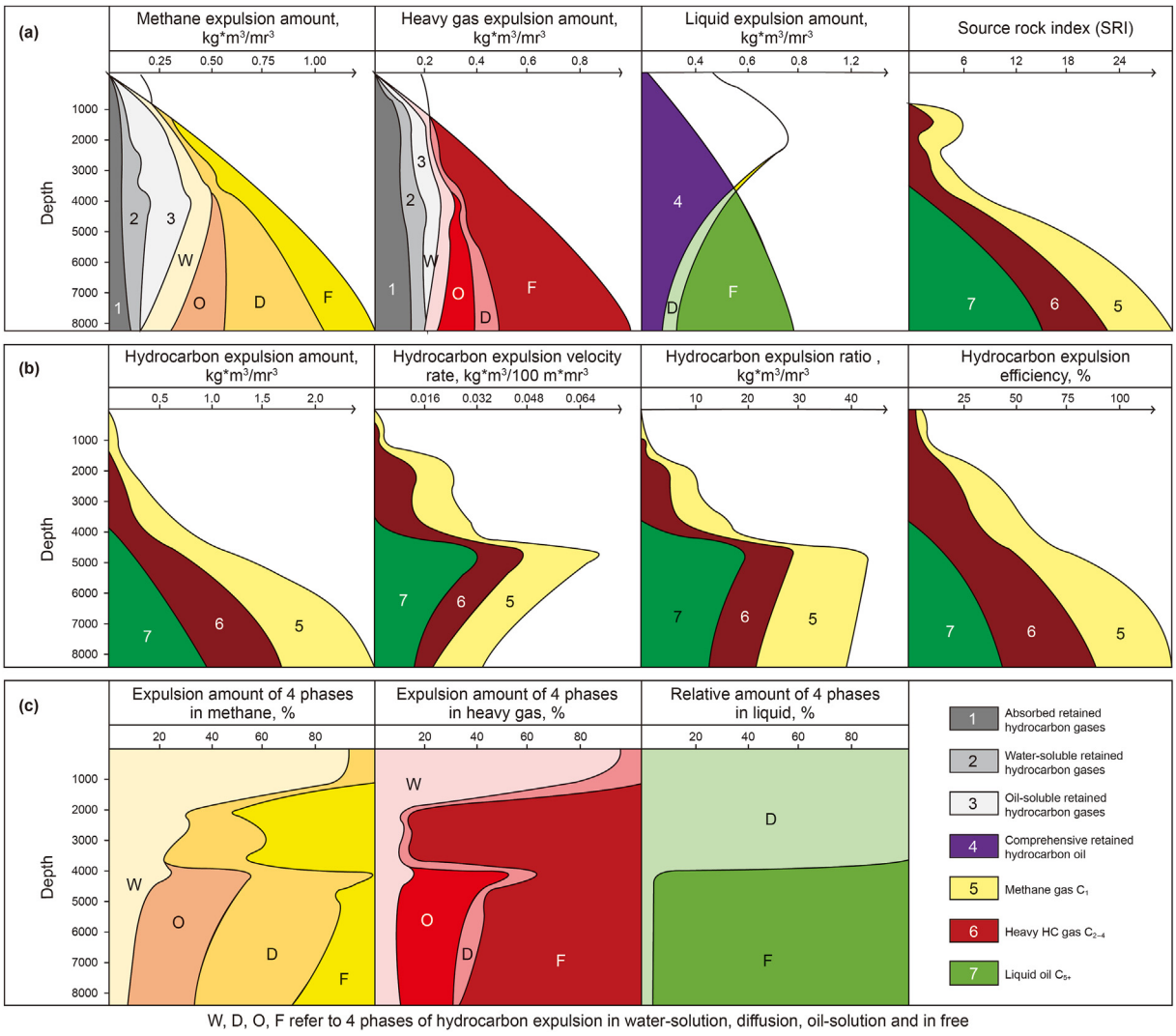

Fig. 6. Case study of the numerical simulation results on hydrocarbon generation, retention, and expulsion in four different phases for the source rocks in the Tarim Basin with the following essential parameters: $TOC = 1.5\%$, $KTI = 85$, $R_o = 1.8\%$, $H = 200$ m, $GT = 2.5$ °C/100 m. (a) Variations of hydrocarbon generation, retention, and expulsion per cubic meter of source rocks with increasing depth for methane, heavy hydrocarbon gas, liquid, and source-rock index (*SRI*). (b) Variation of the hydrocarbon expulsion characteristics of the hydrocarbon expulsion amount, hydrocarbon expulsion velocity rate, hydrocarbon expulsion rate, and hydrocarbon expulsion efficiency. (c) Variations of the relative oil/gas amounts expelled in four different phases from source rocks, including methane, heavy gas, and liquid hydrocarbons. W, D, O, and F represent the relative amounts of hydrocarbons expelled from the source rocks in the water-soluble, diffusion, oil-solution, and free phases, respectively.

The first stage is from the deposition of source rocks at the beginning to the HET underground, dominated by the compaction of overburdened strata. Most of the oil and gas were expelled in water-soluble and diffusion phases, and the relative contributions of compaction (F6), diffusion (F1), thermal expansion (F2–F5), and product volume expansion (F7–F8) are approximately 40%, 25%, 20%, and 15%, respectively. This is unfavorable for oil/gas migration and accumulation in reservoir layers because the generated oil/gas amounts are insufficient to accomplish the retention of oil and gas in source rocks and oil/gas could not be expelled massively in the free phase. The accumulative expelled oil/gas amounts in this stage is less than 10% of the total amount, primarily because of the low solubility of oil/gas in water, the small diffusion coefficient of oil/gas through the rocks, and the very limited oil and gas amounts generated by the source rocks.

The second stage is from HET to the liquid hydrocarbon expulsion depth (LHED), where both oil and gas were expelled from the source rocks in four phases. Most (65%–85%) oil and gas were expelled in the free phase (with some gas migrating in the oil-solution phase), dominated by multidriving forces, i.e., CPD, thermal expansion, and product volume expansion, and others. Their relative contributions to oil/gas expulsion are 40%, 30%, 20%, and 10%, respectively. The source-rock distribution area with developed sapropel-type organic parent material is conducive to the formation of pure oil reservoirs where natural gas is dissolved. The source-rock distribution area with developed humic-type organic parent material is favorable for the formation of pure gas reservoirs. Meanwhile, the distribution of source rocks with transitional-type organic parent material is favorable for the formation of oil and gas reservoirs.

The third stage begins with source rocks entering LHED and lasts to the active source-rock depth limit, indicating the end of hydrocarbon generation and expulsion (Pang et al., 2020). Natural gas with little liquid oil is expelled from the source rocks in the free phase. More than 50% of the natural gas is expelled in this stage via CPD, and the relative hydrocarbon amounts expelled through diffusion, thermal expansion of rocks and fluids, and compaction of overlying strata are less than 5%, 10%, and 15%, respectively.

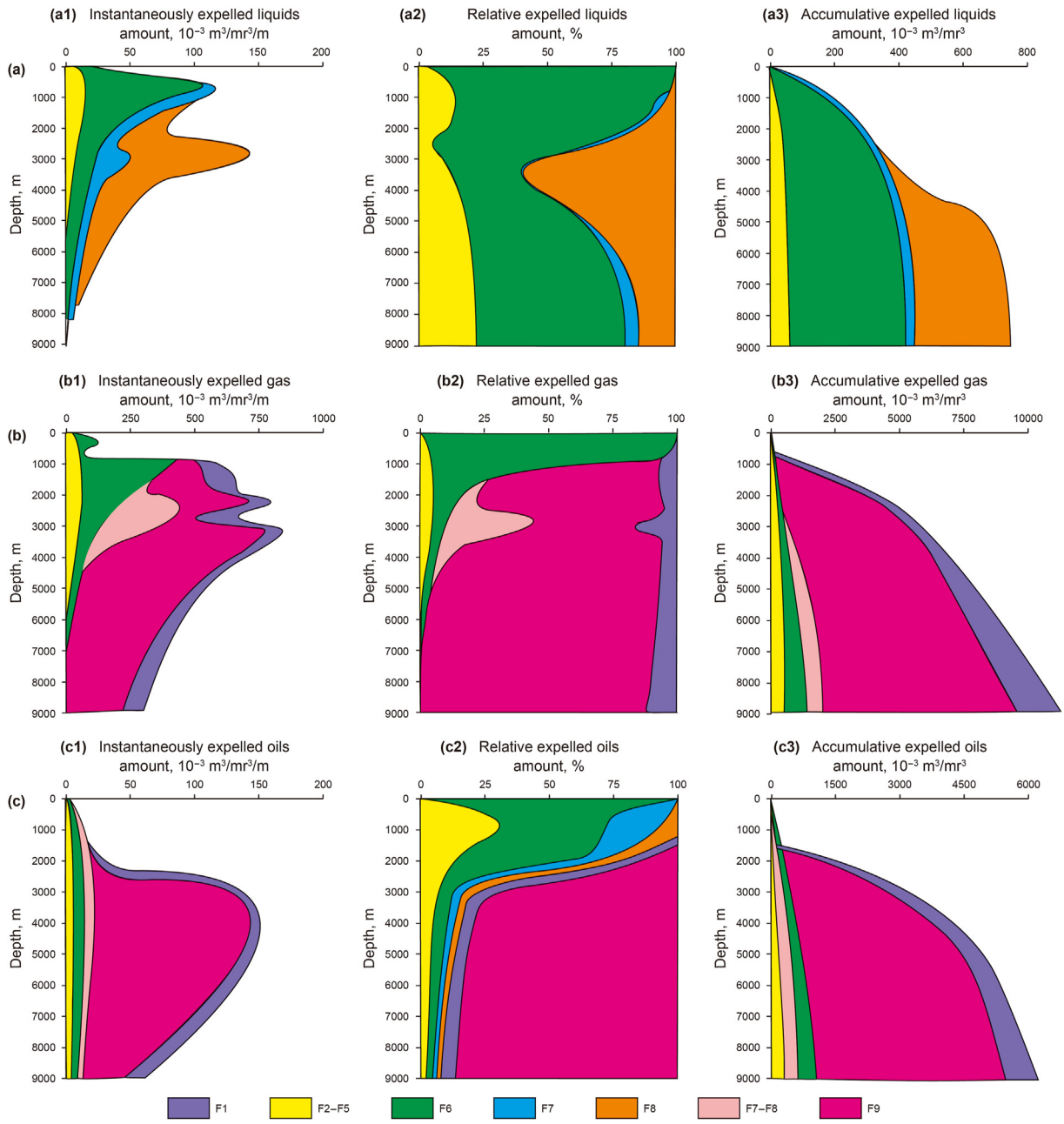

Fig. 7. Numerical simulation results for the fluid expulsion of water, oil, and gas due to the nine driving forces from the source rocks and their relative contributions with increasing burial depth. (a) Variation characteristics of the expelled liquid amounts from the source rocks, including instantaneous expelled liquid amounts (a1), relative expelled liquid amounts (a2), and accumulative expelled liquid amounts (a3). (b) Variation characteristics of the expelled gas amount, including instantaneous expelled gas amounts (b1), relative expelled gas amounts (b2), and accumulative expelled gas amounts (b3). (c) Variation characteristics of the expelled oil amount, including instantaneous expelled oil amounts (c1), relative expelled oil amounts (c2), and accumulative expelled oil amounts (c3). F1 denotes the diffusion of hydrocarbons. F2–F5 denote the thermal volume expansions of mineral skeleton, water, liquid oil, and natural gas. F6 denotes the compaction caused by overlying strata. F7 and F8 denote the product volume expansions induced via clay dehydration and kerogen transformation to oil/gas. F9 denotes the capillary pressure difference (CPD).

In summary, CPD is the most important driving force for hydrocarbon expulsion from effective source rocks. Its relative contribution is more than 50% with a porosity of <10% ± 2%, which increases with increasing depth. Meanwhile, the other eight driving forces are important for hydrocarbon expulsion but are limited by the evolution stage of source rocks and the phases of the expelled hydrocarbons. Their total contributions to hydrocarbon expulsion are less than 50%. These results imply that the deeper the source rocks, the more important CPD becomes for tight hydrocarbon reservoir accumulation.

5. Discussion

For a long time, overpressure has been considered the main driving force for hydrocarbon expulsion from source rocks (Dickinson, 1953; Hunt, 1990; Osborne and Swarbrick, 1997; Hao, 2005; Jiang et al., 2016). During the formation and evolution of sedimentary basins, many physical and chemical processes can produce overpressure (Holbrook et al., 1995; Tingay et al., 2013). It is generally believed that the main reasons for large-scale overpressure in sedimentary basins are compaction, fluid expansion

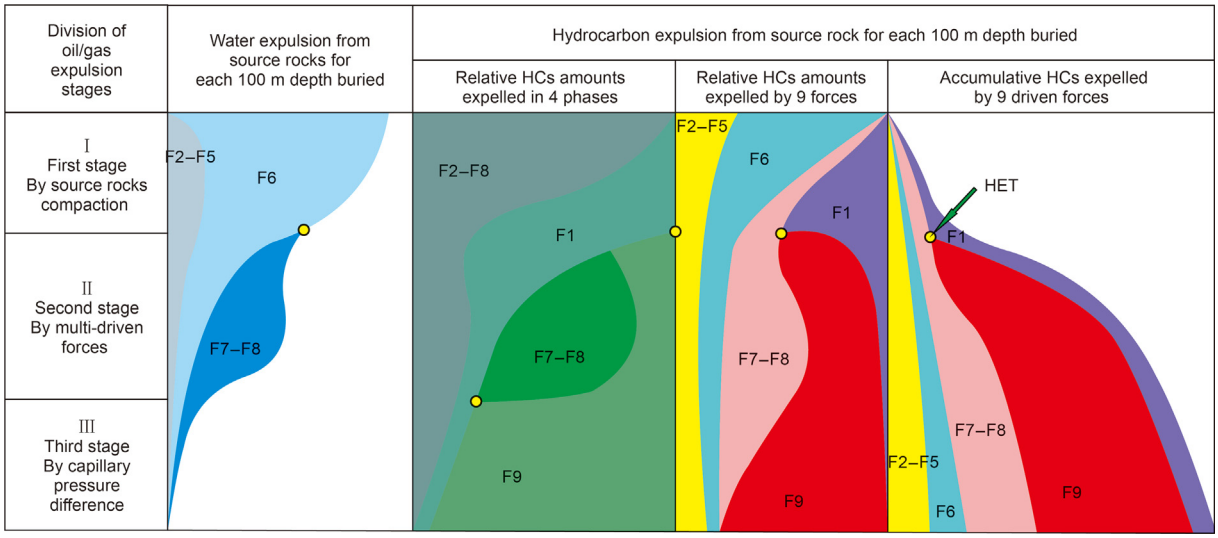

Fig. 8. Dynamic model for hydrocarbon expulsion in four phases from source rocks and the stage division based on the variation characteristics of the driving forces' contributions with increasing depth. The F_i definitions are the same as those presented in Fig. 7.

and kerogen conversion (Hao, 2005; Jiang et al., 2016). However, the hydrocarbon expulsion of source rocks is controlled by complicated geological factors, and their contributions to hydrocarbon expulsion at different stages vary greatly. Therefore, it is necessary to establish a unified model to study the dynamics of hydrocarbon expulsion in the process of hydrocarbon expulsion from source rocks. In this study, a model for evaluating the contribution of multiple dynamics to hydrocarbon expulsion was established and applied to the Cambrian source rocks in the Tarim Basin. The results demonstrate that CPD is the most important contributor to hydrocarbon expulsion in tight reservoirs, especially in the deep formation. This may be related to the four characteristics of CPD: (1) always coexists between source rocks and surrounding reservoir layers due to the difference in their pore throat (Pang et al., 2021a); (2) is continuously and uninterruptedly active (Jia et al., 2021); (3) irreversible migration direction from smaller to larger throats (England et al., 1987); and (4) irreplaceable role in the accumulation of oil/gas in deep and tight reservoirs where the effects of other driving forces greatly weaken and almost disappear (Magara, 1987).

It should be noted that the result of the model changes due to different geological conditions. Most hydrocarbons are generated in source rocks and primarily accumulate in source rocks to form shale oil or gas resources (Liu et al., 2017). However, in the Tarim Basin, fractures and secondary pores generated by tectonic movement improve the quality of the reservoirs, increasing the pore throat radius in the reservoirs and generating large CPD (Pang et al., 2016). And the exploration results in the Tarim Basin demonstrate that 92% of the proven reserves are distributed in the deep tight reservoirs developed with fractures and secondary pores (Fig. 9; Shen et al., 2018), where there exists large CPD between the source rocks and surrounding rocks. The exploration results confirm the reliability of this model. However, when source rocks are in contact with reservoirs with low porosity and permeability, the CPD makes

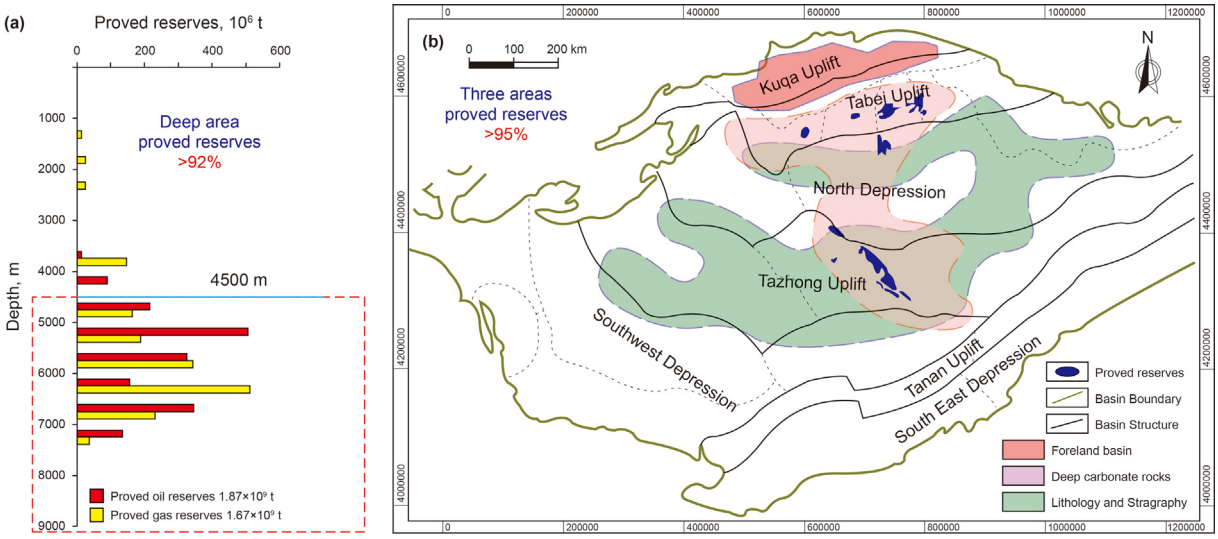

Fig. 9. Distribution characteristics of the proven reserves of oil and gas in the Tarim Basin. (a) The vertical distribution indicates that 92% of the proven oil and gas reserves are in deep and tight reservoirs with depths of >4500 m. (b) Favorable exploration areas include three types: complex structures in the foreland basin, deep carbonate rocks, and lithologic and stratigraphic reservoirs in the platform basin. All the discovered oil and gas reservoirs and 95% of the proven reserves are distributed in the favorable exploration area.

a relatively small contribution to hydrocarbon expulsion. Therefore, in order to better understand the dynamic mechanism of hydrocarbon expulsion of source rocks in different basins, it is necessary to establish models for different source rocks. In addition, some parameters in this model are obtained from laboratory conditions, which may have slight errors compared with the parameters in the geological conditions.

6. Conclusions

1. Continuous tight oil/gas reservoirs are widely developed in deep petroliferous basins, and the main dynamics associated with the oil/gas expulsion from source rocks can be divided into five types (and nine driving forces). Under the combined action of various dynamics, hydrocarbons are expelled from the source rocks in four phases. Based on the principle of material balance, a numerical model is proposed in this study to evaluate the relative contribution of different dynamics for hydrocarbon expulsion from the source rocks. The model can obtain the relative contribution of each dynamic on hydrocarbon expulsion in the geological history.
2. This numerical model is applied to the Cambrian source rocks in the Tarim Basin. Among the driving forces, the simulation results demonstrate that the CPD is the most important driving force for hydrocarbon expulsion in the Cambrian source rocks, expelling a large amount of hydrocarbons in the free phase. The contributions of compaction, product volume expansion, and thermal expansion to hydrocarbon expulsion are relatively small. The relative contribution of diffusion to the expulsion of hydrocarbons is the smallest, mainly expelling hydrocarbons in the diffusion phase.
3. The process of hydrocarbon expulsion can be divided into three stages. The first stage is when hydrocarbons are expelled via compaction and diffusion in the water-soluble and diffusion phases, which is not beneficial for oil and gas accumulation. The second stage features a large amount of hydrocarbon expulsion, and it expels hydrocarbons in various phases via CPD and product volume expansion. The third stage is when gas is expelled in the free phase due to volume thermal expansion and CPD. The second and third stages are the most important stages of hydrocarbon expulsion from the source rocks.

Acknowledgements

This study is financially supported by the Joint Fund of the National Natural Science Foundation of China under grant number U19B6003-02-04, the Science Foundation of China University of Petroleum, Beijing, under grant number 2462020BJRC005 and 2462022YXZZ007, the National Natural Science Foundation of China under grant number 42102145, and the China National Petroleum Corporation's "14th Five-Year Plan" major scientific projecs under grant number 2021DJ0101. We highly appreciate the leaders and experts of the Tarim Oilfield Company, PetroChina, as well as the scientists from our research group. Further, we are grateful to Xinhe Shao, Kun Zhang, and Wenyang Wang, who contributed immensely to improving this manuscript.

References

SPE, AAPG, WPC, et al, 2007. Petroleum Resources Management System. IEA, Washington DC.

Bao, Y.S., Zhang, L.Y., Zhang, S.C., et al., 2017. Effectiveness of capillary pressure on the primary migration of oil and its accumulation. Geol. J. China Univ. 23, 296–303. https://doi.org/10.16108/j.issn1006-7493.2016211, 02(in Chinese).

Barker, C., 1980. Primary migration: the importance of water-mineral-organic matter interactions in the source rock. AAPG Bull. 34, 1–19. https://doi.org/10.1306/St10411C2.

Behar, F., Beaumont, V., De, B., et al., 2001. Rock-eval 6 technology: performances and developments. Oil Gas Sci. Technol. 56 (2), 111–134. https://doi.org/10.2516/OGST:2001013.

Berg, R.R., 1975. Capillary pressures in stratigraphic traps. AAPG Bull. 59 (6), 939–956. https://doi.org/10.1306/83D91EF7-16C7-11D7-8645000102C1865D.

Bruce, C., 1984. Smectite dehydration; its relation to structural development and hydrocarbon accumulation in northern gulf of Mexico basin. AAPG Bull. 68 (6), 673–683. https://doi.org/10.1007/BF01081374.

Chen, F.J., Tian, S.C., 1989. Compaction and Oil and Gas Migration. China University of Geoscience Press.

Chen, J., Pang, X., Pang, H., et al., 2018. Hydrocarbon evaporative loss evaluation of lacustrine shale oil based on mass balance method: permian Lucaogou Formation in Jimusaer Depression, Junggar Basin. Mar. Petrol. Geol. 191, 422–431. https://doi.org/10.1016/j.marpetgeo.2018.01.021.

Danial, J., Bustin, R., 2007. Impact of mass balance calculations on adsorption capacities in microporous shale gas reservoirs. Fuel 86 (17–18), 2696–2706. https://doi.org/10.1016/j.fuel.2007.02.036.

David, L., Janos, U., Lisa, N., et al., 1997. The influence of swelling clays on the deformation of mudrocks. Int. J. Rock Mech. Min. 34 (3–4). https://doi.org/10.1016/S0148-9062(97)00224-6, 364-364.

Dickey, P.A., 1975. Possible primary migration of oil from source rock in oil phase. AAPG (Am. Assoc. Pet. Geol.) Bull. 59 (2), 337–345. https://doi.org/10.1306/83D91C8B-16C7-11D7-8645000102C1865D.

Dickinson, G., 1953. Geological aspects of abnormal reservoir pressures in Gulf Coast Louisiana. AAPG (Am. Assoc. Pet. Geol.) Bull. 37 (8), 410–432. https://doi.org/10.1306/5CEADC6B-16BB-11D7-8645000102C1865D.

Du, R., 1981. Stress fields: a key to oil migration. AAPG Bull. 65 (1), 168–174. https://doi.org/10.1306/2F919774-16CE-11D7-8645000102C1865D.

England, W., Mackenzie, A., Mann, D., et al., 1987. The movement and entrapment of petroleum fluids in the subsurface. J. Geol. Soc. London 144, 327–347. https://doi.org/10.1144/gsjgs.144.2.0327.

Espitalie, J., Madec, M., Tissot, B., 1980. Role of mineral matrix in kerogen pyrolysis; influence on petroleum generation and migration. AAPG Bull. 64 (1), 59–66. https://doi.org/10.1007/BF01081857.

Germann, P., 2018. Viscosity-The weak link between Darcy's law and Richards' capillary flow. Hydrol. Process. 32 (9). https://doi.org/10.1002/hyp.11450, 1166-1120.

Han, J.F., Zhang, H.Z., Yu, H.F., et al., 2012. Hydrocarbon accumulation characteristic and exploration on large marine carbonate condensate field in Tazhong Uplift. Acta Petrol. Sin. 28 (3), 769–782. CNKI:SUN:YSXB.0.2012-03-007 (in Chinese).

Hao, F., 2005. Kinetics of Hydrocarbon Generation and Mechanisms of Petroleum Accumulation in Overpressure Basins. Science Press, Beijing (in Chinese).

He, X., Gui, Y., Xie, J., et al., 2020. A DFT study of dissolved gas (C_2H_2, H_2, CH_4) detection in oil on CuO-modified BNNT. Appl. Surf. Sci. 500, 144030. https://doi.org/10.1016/j.apsusc.2019.144030.

Holbrook, P.W., Maggiori, D.A., Hensley, R., 1995. Real-time pore pressure and fracture gradient evaluation in all sedimentary lithologies. SPE Form. Eval. 10 (4), 215–222. https://doi.org/10.2118/26791-PA.

Hu, T., Pang, X.Q., Jiang, F.J., et al., 2022. Dynamic continuous hydrocarbon accumulation (DCHA): Existing theories and a new unified accumulation model. Earth-Science Reviews 232, 104109. https://doi.org/10.1016/j.earscirev.2022.104109.

Hu, Z.Y., Sun, D., Hu, Y.Y., et al., 2015. The controlling effect of carbonate fault system on reservoirs: a case study in the 3rd block of Tazhong area. Nat. Gas Geosci. 26, 97–106. https://doi.org/10.11764/j.issn.1672-1926.2015.S1.009.

Huang, H.P., Zhang, S.C., Su, J., 2016. Palaeozoic oil–source correlation in the Tarim Basin, NW China: a review. Org. Geochem. 94, 32–46. https://doi.org/10.1016/j.orggeochem.2016.01.008.

Hubbert, M.K., 1953. Entrapment of petroleum under hydrodynamic conditions. AAPG (Am. Assoc. Pet. Geol.) Bull. 37 (8), 1954–2026. https://doi.org/10.1306/5CEADD61-16BB-11D7-8645000102C1865D.

Hunt, J.M., 1979. Petroleum Geochemistry and Geology, lst ed. W. H. Freeman and Company, New York.

Hunt, J.M., 1990. Generation and migration of petroleum from abnormally pressured fluid compartments. AAPG (Am. Assoc. Pet. Geol.) Bull. 74 (1), 1–12. https://doi.org/10.1029/JB095iB01p00649.

Jarvie, D.M., 2012. Shale Resource Systems for Oil and Gas: Part 2: Shale-Oil Resource Systems. BREYER J A. Shale Reservoirs: Giant Resources for the 21st Century. AAPG, Tulsa, pp. 89–119.

Jia, C.Z., 2017. On the breakthrough of unconventional oil and gas to classical oil and gas geology theory and its significance. Petrol. Explor. Dev. 44 (1), 1–11. https://doi.org/10.1016/S1876-3804(17)30002-2.

Jia, C.Z., Pang, X.Q., Song, Y., 2021. The mechanism of unconventional hydrocarbon formation: hydrocarbon self-sealing and intermolecular forces. Petrol. Explor. Dev. 48 (3), 507–526. https://doi.org/10.1016/S1876-3804(21)60042-3.

Jiang, F., Pang, X., Bai, J., et al., 2016. Comprehensive assessment of source rocks in the Bohai Sea area, eastern China. AAPG Bull. 100 (6), 969–1002. https://doi.org/10.1306/02101613092.

Jiang, Y.L., Wang, X., Yu, Q.Q., et al., 2016. Pressure field characteristics of petroliferous depressions and its relationship with hydrocarbon enrichment in Bohai Bay Basin. Acta Petrol. Sin. 37 (11), 1361–1369. https://doi.org/10.7623/syxb201611004 (in Chinese).

Jiang, H., Pang, X.Q., Yu, R., et al., 2017. Lower limit of hydrocarbon accumulation in the Kuqa depression, Tarim Basin, NW China. Geol. J. 52, 141–153. https://

doi.org/10.1002/gj.2740.
Johnson, R.H., 1912; Mar 22. The accumulation of oil and gas in sandstone. Science 35 (899), 458–459. https://doi.org/10.1126/science.35.899.458.
Lan, X.D., Lv, X.X., Zhu, Y.M., 2015. The geometry and origin of strike-slip faults cutting the Tazhong low rise megaanticline (central uplift, Tarim Basin, China) and their control on hydrocarbon distribution in carbonate reservoirs. J. Nat. Gas Sci. Eng. 22, 633–645. https://doi.org/10.1016/j.jngse.2014.12.030.
Lee, W., Kang, P., Kim, A., et al., 2018. Impact of surface porosity on water flux and structural parameter in forward osmosis. Desalination 439, 46–57. https://doi.org/10.1016/j.desal.2018.03.027.
Lerche, I., 1990. Basin Analysis: Quantitative Methods. Academic Press, San Diego.
Leythaeuser, D., Schaefer, R.G., Yukler, A., 1982. Role of diffusion in primary migration of hydrocarbons. AAPG Bull. 66 (4), 408–429. https://doi.org/10.1007/BF01081377.
Leythaeuser, D., Mackenzie, A., Schaefer, R., et al., 1984. A novel approach for recognition and quantification of hydrocarbon migration effects in shale-sandstone sequences. AAPG Bull. 68 (2), 196–219. https://doi.org/10.1002/esp.3290080607.
Li, M.C., 2004. Migration of Oil and Natural Gas. Petroleum Industry Press (in Chinese).
Li, S.M., Pang, X.Q., Jin, Z.J., et al., 2010. Petroleum source in the Tazhong Uplift, Tarim Basin: new insights from geochemical and fluid inclusion data. Org. Geochem. 41, 531–553. https://doi.org/10.1016/j.orggeochem.2010.02.018.
Li, S.M., Amrani, A., Pang, X.Q., 2015. Origin and quantitative source assessment of deep oils in the Tazhong Uplift, Tarim Basin. Org. Geochem. 78, 1–22. https://doi.org/10.1016/j.orggeochem.2014.10.004.
Li, C., Zhen, K., Hao, Y., et al., 2018. Effect of dissolved gases in natural water on the flotation behavior of coal. Fuel 233 (DEC.1), 604–609. https://doi.org/10.1016/j.fuel.2018.06.104.
Lindgreen, H., 1985. Diagenesis and primary migration in upper Jurassic claystone source rocks in Northsea. AAPG Bull. 69 (4), 525–536. https://doi.org/10.1306/ad462524-16f7-11d7-8645000102c1865d.
Liu, W.B., Ju, Z.X., Han, J.F., 2015. Hydrocarbon accumulation characteristics and enrichment law of various carbonate layer series of the Ordovician system in III-zone, central Tarim Basin. Nat. Gas Geosci. 1, 125–137. https://doi.org/10.11764/j.issn.1672-1926.2015.S2.0125.
Liu, Y.K., Xiong, Y.Q., Li, Y., et al., 2017. Effects of oil expulsion and pressure on nanopore development in highly mature shale: evidence from a pyrolysis study of the Eocene Maoming oil shale, south China. Mar. Petrol. Geol. 86, 526–536. https://doi.org/10.1016/j.marpetgeo.2017.06.012.
Magara, K., 1975a. Reevaluation of montmorillonite dehydration as cause of abnormal pressure and hydrocarbon migration. AAPG Bull. 59 (2), 292–302. https://doi.org/10.1007/BF01134160.
Magara, K., 1975b. Importance of aquathermal pressuring effect in Gulf Coast. AAPG Bull. 59 (10), 2037–2045. https://doi.org/10.1306/83D921DB-16C7-11D7-8645000102C1865D.
Magara, K., 1976. Thickness of removed sediments paleopore pressure and paleotemperature south western part of western Canada Basin. AAPG Bull. 60, 554–565. https://doi.org/10.1306/83D92401-16C7-11D7-8645000102C1865D.
Magara, K., 1978. The significance of the expulsion of water in oil-phase primary migration. Bull. Can. Petrol. Geol. 26 (1), 123–131. https://doi.org/10.1007/978-1-4612-1980-4_7.
Magara, K., 1981. Mechanisms of nature fracturing in a sedimentary basin. AAPG Bull. 65 (1), 123–132. https://doi.org/10.1306/2F919783-16CE-11D7-8645000102C1865D.
Magara, K., 1987. Compaction and Fluid Migration. Elsevier, Amsterdam.
McAulife, C.D., 1979. Oil/gas migration-Chemical and physical constraints. AAPG Bull. 63 (5), 767–781. https://doi.org/10.1306/2f9182cf-16ce-11d7-8645000102c1865d.
Neglia, S., 1979. Migration of fluids in sedimentary basins. AAPG Bull. 63 (4), 573–597. https://doi.org/10.1306/2f918194-16ce-11d7-8645000102c1865d.
Olgaard, D.L., Urai, J., Dell'Angelo, L.N., et al., 1997. The influence of swelling clays on the deformation of mudrocks. Int. J. Rock Mech. Min. Sci. 34 (3–4). https://doi.org/10.1016/S0148-9062(97)00224-6, 364-364.
Osborne, M.J., Swarbrick, R.E., 1997. Mechanisms for generating overpressure in sedimentary basins: a reevaluation. AAPG Bull. 81 (6), 1023–1041. https://doi.org/10.1093/ietcom/e90-b.2.425.
Pang, X., Chen, Z., Chen, F., 1992. The Optimum Modelling of the Amount of Oil/gases Formed by the Kerogens in Their Evolution Based on the Material Balance Principle. Petroleum Exploration and Development, pp. 23–31, 01CNKI:SUN:SKYK.0.1992-01-003 (in Chinese).
Pang, X., Chen, Z., Chen, F., 1993. Study on Numerical Simulation of Geological History, Thermal History, Hydrocarbon Generation-Expulsion History and Quantitative Evaluation of Hydrocarbon Source Rocks in Petroliferous Basins. Geological Publishing House, Beijing (in Chinese).
Pang, X.Q., Jin, Z.J., Zuo, S.J., 2000. Dynamics, models and classification of hydrocarbon accumulation. Earth Sci. Front. 507–514. https://doi.org/10.3321/j.issn:1005-2321.2000.04.020, 04.
Pang, X.Q., Lerche, I., Wang, Y.C., et al., 2001. Theoretical Research and Application of Hydrocarbon Expulsion Threshold for Coal-Measure Source Rocks. Petroleum Industry Press, Beijing (in Chinese).
Pang, X.Q., Jin, Z.J., Jiang, Z.X., et al., 2003. Critical condition for gas accumulation in the deep basin trap and physical modeling. Nat. Gas Geosci. 14 (3), 207–214. https://doi.org/10.3969/j.issn.1672-1926.2003.03.011 (in Chinese).
Pang, X., Li, M., Li, S., et al., 2005. Geochemistry of petroleum systems in the Niuzhuang south slope of Bohai Bay basin: Part 3. Estimating hydrocarbon expulsion from the Shahejie formation. Org. Geochem. 36 (4), 497–510. https://doi.org/10.1016/j.orggeochem.2004.12.001.
Pang, X.Q., Chen, J.Q., Li, S.M., et al., 2016. Evaluation method and application of the relative contribution of marine hydrocarbon source rocks in the Tarim Basin: a case study from the Tazhong area. Mar. Petrol. Geol. 77, 1–18. https://doi.org/10.1016/j.marpetgeo.2016.05.023.
Pang, X.Q., Jia, C.Z., Zhang, K., et al., 2020. The dead line for oil and gas and implication for fossil resource prediction. Earth Syst. Sci. Data 12, 577–590. https://doi.org/10.5194/essd-12-577-2020.
Pang, X.Q., Jia, C.Z., Wang, W.Y., et al., 2021a. Buoyance-driven hydrocarbon accumulation depth and its implication for unconventional resource prediction. Geosci. Front. 12 (4), 101133. https://doi.org/10.1016/j.gsf.2020.11.019.
Pang, X., Shao, X., Li, M., et al., 2021b. Correlation and difference between conventional and unconventional reservoirs and their unified genetic classification. Gondwana Res. 97 (6). https://doi.org/10.1016/j.gr.2021.04.011.
Pittman, E.D., 1992. Relationship of porosity and permeability to various parameters derived from mercury injection-capillary pressure curves for sandstone. AAPG Bull. 76, 191–198. https://doi.org/10.1306/BDFF87A4-1718-11D7-8645000102C1865D.
Price, L., 1976. Aqueous solubility of petroleum as applied to its origin and primary migration. AAPG Bull. 60 (2), 213–244. https://doi.org/10.1306/83d922a8-16c7-11d7-8645000102c1865d.
Qiao, J., Zeng, J., Jiang, S., et al., 2019. Heterogeneity of reservoir quality and gas accumulation in tight sandstone reservoirs revealed by pore structure characterization and physical simulation. Fuel 253, 1300–1316. https://doi.org/10.1016/j.fuel.2019.05.112.
Qu, Z., Yin, Y., Wang, H., et al., 2020. Pore-scale investigation on coupled diffusion mechanisms of free and adsorbed gases in nanoporous organic matter. Fuel 260, 116423. https://doi.org/10.1016/j.fuel.2019.116423.
Rexer, T.F.T., Benham, M.J., Aplin, A.C., et al., 2013. Methane adsorption on shale under simulated geological temperature and pressure conditions. Energy Fuels 27 (6), 3099–3109. https://doi.org/10.1021/ef400381v.
Rose, W., 2001. Modeling forced versus spontaneous capillary imbibition processes commonly occurring in porous sediments. J. Petrol. Sci. Eng. 30 (3–4), 155–166. https://doi.org/10.1016/S0920-4105(01)00111-5.
Rouchet, J.D., 1981. Stress fields, A key to oil migration. AAPG Bull. 65 (1), 74–85. https://doi.org/10.1306/2F919774-16CE-11D7-8645000102C1865D.
Shen, W., Chen, J., Wang, Y., et al., 2018. The origin, migration and accumulation of the Ordovician gas in the Tazhong III region, Tarim Basin, NW China. Mar. Petrol. Geol. 101, 55–77. https://doi.org/10.1016/j.marpetgeo.2018.11.031.
Song, Y., Ma, X.S., Liu, S.B., et al., 2019. Reservoir formation conditions and key technologies for exploration and development of Qinshui coalbed methane field. Acta Pet. Sin. 40 (5), 621–634. https://doi.org/10.7623/syxb201905012 (in Chinese).
Stainforth, J.G., Reinders, J.E.A., 1990. Primary migration of hydrocarbons by diffusion through organic matter networks, and its effect on oil and gas generation. Org. Geochem. 16 (1–3), 61–74. https://doi.org/10.1016/0146-6380(90)90026-V.
Thomas, M.M., Clouse, J.A., 1990. Primary migration by diffusion through kerogen: II. Hydrocarbon diffusivities in kerogen. Geochem. Cosmochim. Acta 54, 2781–2792. https://doi.org/10.1016/0016-7037(90)90012-A.
Tingay, M.R.P., Hillis, R.R., Swarbrick, R.E., et al., 2013. Origin for overpressure generation by kerogen-to-gas maturation in the northern Malay Basin. AAPG Bull. 97 (4), 639–672. https://doi.org/10.1306/09041212032.
Tissot, B., Welte, D., 1978. Petroleum Formation and Occurrence. Springer-Verlag, Berlin.
Tong, X.G., Zhang, G.Y., Wang, Z.M., et al., 2018. Potential and distribution of global oil and gas resources. Petrol. Explor. Dev. 45, 727–736. https://doi.org/10.11698/PED.2018.04.19, 04.
Vernik, L., Landis, C., 1996. Elastic anisotropy of source rocks: implications for hydrocarbon generation and primary Migration1. AAPG Bull. 80 (4), 531–544. https://doi.org/10.1306/64ed8836-1724-11d7-8645000102c1865d.
Wang, E.Z., Feng, Y., Guo, T.L., et al., 2022. Oil content and resource quality evaluation methods for lacustrine shale: A review and a novel three-dimensional quality evaluation model. Earth-Science Reviews 232, 104134. https://doi.org/10.1016/j.earscirev.2022.104134.
Yu, S., Pan, C.C., Wang, J.J., et al., 2012. Correlation of crude oils and oil components from reservoirs and source rocks using carbon isotopic compositions of individual nalkanes in the Tazhong and Tabei Uplift of the Tarim Basin, China. Org. Geochem. 52, 67–80. https://doi.org/10.1016/j.orggeochem.2012.09.002.
Zheng, M., Li, J., Wu, X., et al., 2019. Potential of oil and natural gas resources of main hydrocarbon-bearing basins and key exploration fields in China. Earth Sci. 44, 833–847. https://doi.org/10.3799/dqkx.2019.957, 03.
Zheng, D., Pang, X., Zhou, L., et al., 2020. Critical conditions of tight oil charging and determination of the lower limits of petrophysical properties for effective tight

reservoirs: a case study from the Fengcheng Formation in the Fengcheng area, Junggar Basin. J. Petrol. Sci. Eng. 190, 107135. https://doi.org/10.1016/j.petrol.2020.107135.
Zhu, G.Y., Yang, H.J., Su, J., et al., 2012. New progress of marine hydrocarbon geological theory in China. Acta Petrol. Sin. 3, 722–738. https://doi.org/10.2110/palo.2011.p11-036r.
Zou, C.N., 2014. Unconventional Petroleum Geology. Geological Publishing House, Beijing (in Chinese).
Zou, C.N., Zhu, R.K., Wu, S.T., 2012. Conventional and unconventional hydrocarbon accumulations: taking tight oil and tight gas in China as an instance. Acta Pet. Sin. 33 (2), 173–187. CNKI:SUN:SYXB.0.2012-02-002.